Poly(2-methyl-2-oxazoline) conjugates with doxorubicin: From synthesis of high drug loading water-soluble constructs to in vitro anti-cancer properties

Ondrej Sedlacek,[†,*] Alexandra Van Driessche,[‡] Annemiek Uvyn,[‡] Bruno G. De Geest,[‡] Richard Hoogenboom[†,*]

[†]Supramolecular Chemistry Group, Centre of Macromolecular Chemistry (CMaC), Department of Organic and Macromolecular Chemistry, Ghent University, Krijgslaan 281 S4, B-9000 Ghent, Belgium

[‡]Department of Pharmaceutics and Cancer Research Institute Ghent (CRIG), Ghent University, 9000 Ghent, Belgium

E-mail: richard.hoogenboom@ugent.be

TOC Figure

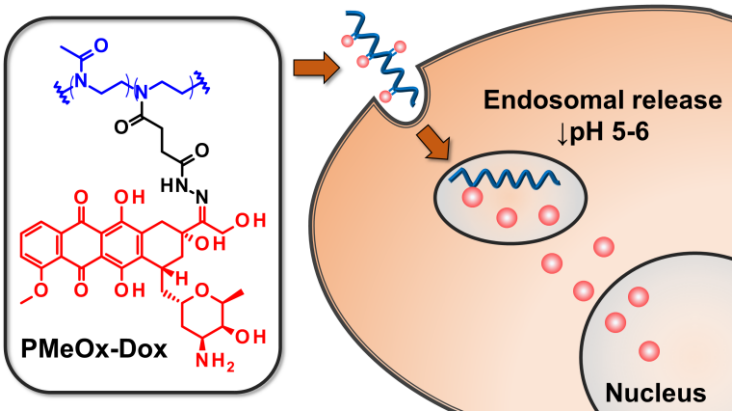

Abstract

Poly(2-oxazoline)s represent an emerging class of polymers with increasing potential in biomedical sciences. To date, most of the work on poly(2-oxazoline)-drug conjugates focused on poly(2-ethyl-2-oxazoline) (PEtOx), a biocompatible water-soluble polymer with biological properties similar to polyethylene glycol. However, the more hydrophilic poly(2-methyl-2-oxazoline) (PMeOx) shows better anti-fouling properties than PEtOx and thus indicates greater potential for the construction of polymer therapeutics. Herein, we synthesized for the first time a drug delivery system based on a linear PMeOx with a molar mass that is high enough (40 kDa) to exploit passive accumulation in the tumor by the enhanced permeation and retention effect. The anti-cancer drug doxorubicin is attached to the polymer carrier via an acid-sensitive hydrazone bond, which allows its pH-triggered release in the tumor. The in vitro study demonstrates successful cellular uptake of the PMeOx-doxorubicin conjugate via clathrin-mediated endocytosis, pH-sensitive drug release and high cytotoxicity against B16 melanoma cells. Finally, these properties were critically compared to the analogous systems based on the established PEtOx revealing that the more hydrophilic PMeOx carrier outperforms PEtOx in most of the parameters, showing higher maximal drug loading, superior cellular uptake, better anti-fouling properties, as well as improved in vitro anti-cancer efficiency. The study demonstrates the potential of PMeOx as a versatile platform for synthesis of new drug delivery systems.

KEYWORDS:

polymer therapeutics; polymer-drug conjugate; poly(2-oxazoline); drug delivery

INTRODUCTION

The use of synthetic polymers as anti-cancer drug delivery systems has received substantial attention [1]. Conjugation of cytostatic drugs to a water-soluble polymer carrier often improves their solubility, extends the blood circulation time, results in better therapeutic activity and reduced side-effects [2-6]. When an anti-fouling polymer is used, the drug opsonization by the mononuclear phagocyte system is prevented by the suppression of interactions with proteins and cells, the so-called "stealth-effect". Furthermore, nanoscale drug delivery systems passively accumulate in cancerous tissue due to its leaky vasculature and improperly developed lymphatic system (so-called enhanced permeation and retention, EPR, effect) [7, 8]. The EPR effect increases with increasing size of the polymer conjugate. In the case of non-biodegradable polymer carriers, however, the polymer size should not exceed the renal filtration threshold (reported to be 30-70 kDa depending on the polymer type) to assure gradual excretion by the kidneys. Several synthetic polymers have been studied as platforms for drug delivery systems, particularly poly(ethylene oxide) (PEO) [9], poly(*N*-vinyl-2-pyrrolidone) (PVP) [10] and poly[*N*-(2-hydroxypropyl)methacrylamide] (PHPMA) [11, 12].

Poly(2-alkyl-2-oxazoline)s (PAOx) represent an emerging class of polymers with applications across many scientific disciplines [13-15]. They are synthesized by living cationic ring-opening polymerization (CROP) of 2-alkyl-2-oxazoline monomers initiated by electrophiles (e.g., alkyl halides or tosylates) to provide low-dispersity polymers isostructural to peptides and proteins [16]. The high synthetic versatility of PAOx, resulting from the controlled living character of the CROP, as well as a simple introduction of orthogonal functional groups to both chain-ends by selection of appropriate initiators and/or terminating agents, underlines their potential as a versatile polymer platform for universal use. The hydrophilicity of PAOx depends mainly on the substituent in 2-position of the 2-oxazoline ring. PAOx with the shortest 2-substituent, *e.g.*, poly(2-methyl-2-oxazoline) (PMeOx, **Figure 1**) and poly(2-ethyl-2-oxazoline) (PEtOx), are water-soluble, biocompatible, non-fouling polymers with biological properties often outperforming those of PEO, a polymer widely used in biomedical research [17-21]. While PEO can be modified just on its chain ends, 2-oxazolines can be copolymerized with a wide range of functional monomers, introducing functionalities into the side-chains og the resulting PAOx. This increases the conjugation potential, as well as the possible drug loading of PAOx-drug conjugates.

Despite their undeniable potential for biomedical applications, reports on drug delivery systems based on PAOx are still relatively sparse. They are mostly limited to amphiphilic micellar

systems loaded with anti-cancer drugs by non-covalent hydrophobic interactions [22]. These systems are simple and relatively effective; however, they suffer from the unavoidable non-specific leakage of the drug from the micellar core, which might lead to the hampered therapeutic effectivity and undesired side effects. Several lower-molar mass (< 5 kDa) PEtOx-drug conjugates have also been described, where the cytostatic drug (ciprofloxacin or Ara-C) was covalently connected to the polymer by a relatively stable ester or amide bond, which can limit the drug release in the target tissue [23, 24]. This concept was, however, effective for the construction of PEtOx-rotigotine conjugates for the treatment of Parkinson's disease upon once a week subcutaneous administration and are currently in Phase 1 of clinical trials [25]. The therapeutic potential of polymer-drug conjugates can be enhanced by introducing a stimuli-degradable linker between the drug and the polymer [26-28]. During plasma circulation, the conjugate remains stable and inactive, with the drug linked to its biocompatible polymer carrier. Once it reaches the target location (*i.e.*, tumor tissue or cells), the cytostatic payload is released in a controlled way due to the tumor-specific redox [29], acidobasic [30, 31] or enzymatic conditions [32]. The hydrazone bond represents an effective pH-responsive linker to connect drugs with polymer carriers [33-35]. It features exceptionally high stability at the physiological pH of blood plasma (7.4), while in the acidic environment of tumor tissue (pH = 6 - 7) or after internalization in endosomes (pH as low as 5) the linker is cleaved, and the cytotoxic drug is released in a controlled way.

The potential of PAOx for the construction of drug delivery conjugates was for a long time limited by assumed inability to synthesize polymers with molar mass high enough to fully exploit the EPR effect-based accumulation (~40 kDa). Recently, however, Monnery et al. reported an improved protocol for the synthesis of low-dispersity PEtOx up to 300 kDa [36]. This was followed by the determination of the renal clearance threshold value for PEtOx (~50 kDa) [37], as well as the first high-molar mass PEtOx conjugate with the cytostatic doxorubicin connected via a hydrazone bond [38]. This conjugate was therapeutically effective against EL-4 lymphoma *in vivo* with similar anti-tumor efficacy as analogous established PHPMA-doxorubicin conjugates.

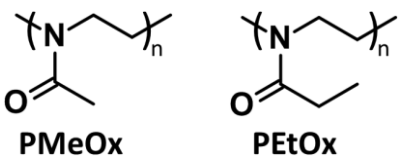

Figure 1. Structures of poly(2-methyl-2-oxazoline) (PMeOx) and poly(2-ethyl-2-oxazoline) (PEtOx).

Recent findings showed that the more hydrophilic poly(2-methyl-2-oxazoline) (PMeOx) outperforms both PEtOx and PEO in anti-fouling properties [39, 40]. Also, the higher hydrophilicity of PMeOx is envisioned to allow higher loading of the hydrophobic drug. These properties, together with the synthetic versatility and modularity, underline the considerable potential of this polymer for construction of drug delivery conjugates. So far, there were no reports on PMeOx-drug conjugates with an appropriate size to exploit passive accumulation by the EPR effect (20 – 50 kDa). The synthesis of high molar mass PMeOx based on the procedure for the synthesis of high-molar mass PEtOx is not possible due to extensive chain transfer during MeOx polymerization [41]. Therefore, an alternative strategy was proposed, consisting in the controlled acetylation of well-defined linear polyethyleneimine resulting in low-dispersity PMeOx with a size of up to 60 kDa [42, 43]. This approach was used herein to synthesize the high molar mass conjugates (MD2-4).

In this study, we report for the first time the synthesis and *in vitro* anti-cancer properties of the water-soluble conjugates based on poly(2-methyl-2-oxazoline) (PMeOx) covalently connected to the cytostatic drug doxorubicin. The drug was connected via the acid-degradable hydrazone bond that assures its controlled release in tumor tissue and endosomes. To demonstrate the biomedical potential of the newly prepared PMeOx conjugates, their *in vitro* anti-cancer properties were critically compared with analogs based on the PEtOx carrier.

EXPERIMENTAL

Materials

2-Methyl-2-oxazoline (MeOx) was purchased from Acros Organics and was distilled from barium oxide and ninhydrin before use. Methyl *p*-toluenesulfonate (MeOTs) was obtained from Sigma-Aldrich and was distilled from CaH_2 before use. Sulfolane (Sigma-Aldrich) was purified by two consecutive distillations, first over barium oxide and then over 2-phenyl-2-oxazolinium tetrafluoroborate. All other chemicals, including *N*,*N*-dimethylacetamide (DMA), triethylamine, hydrazine, chloromethyl succinate, sodium azide, biotin, Atto-655 NHS ester, filipin III, cytochalasin D, chlorpromazine and genistein were purchased from Sigma-Aldrich and were used as received. 2-Phenyl-2-oxazolinium tetrafluoroborate ($HPhOxBF_4$) was synthesized according to the literature procedure [36]. PEtOx homopolymers (PEtOx1, PEtOx2 and PEtOx3 **Table S1**) were synthesized by cationic ring-opening polymerization (CROP) of EtOx at 50 °C according to the published procedure [36]. The high molar mass PMeOx3 was synthesized from PEtOx3 via controlled side-chain hydrolysis and subsequent acetylation of the resulting linear polyethyleneimine (PEI) according to the reference [43]. SKOV-3 and B16 cells were purchased from ATCC. Dulbecco's phosphate-buffered saline (PBS), Dulbecco's modified Eagle Medium (DMEM), Fetal bovine serum (FBS), L-glutamine, penicillin, streptomycin and Hoechst were obtained from Invitrogen. Phalloidin-iFluor 488 Reagent was purchased from Abcam. Rottlerin was purchased from Sanbio.

Synthesis of poly(2-methyl-2-oxazoline) PMeOx2 by CROP of MeOx

The MeOx monomer was first purified by low-temperature static distillation in the presence of an oxazolinium initiator (sacrificial initiator method) as reported before [36]. In the Schlenk flask, MeOx (4.6 g, 101 mmol) and 2-phenyl-2-oxazolinium tetrafluoroborate initiator (39.6 mg, 168 µmol, [M]/[I] = 600) were dissolved under argon atmosphere in freshly distilled sulfolane (13.4 mL) to reach a monomer concentration of 3 M. The reaction mixture was stirred at 60 °C in a glovebox for 2 weeks, followed by termination with solid sodium azide (33 mg, 504 µmol) overnight. The polymerization mixture was diluted with distilled water (10 mL) and dialyzed against the same solvent (molecular weight cut-off, MWCO 3 kDa). PMeOx2 was recovered by freeze-drying as a white powder (yield 71 %). PMeOx1 was synthesized analogously using [M]/[I] = 120.

Synthesis of PMeOx-PEI and PEtOx-PEI

The respective homopolymers (500 mg of PMeOx1-3, respectively PEtOx1-3) were dissolved in 16 % aqueous HCl (c_{pol} = 200 mg mL^{-1}) and stirred at 100 °C in a microwave reactor for 5 min (PMeOx), respectively 6 min (PEtOx). The volatiles were then evaporated under reduced pressure; the solid residue was dissolved in saturated sodium carbonate (10 mL), dialyzed against distilled water (MWCO 3.5 kDa) and recovered by freeze-drying as white powders (yield 88 – 95 %). The degree of hydrolysis (the content of ethyleneimine units) was determined by ^{1}H NMR spectroscopy from the ratio of backbone peak integrals at δ = 2.8 ppm (PEI) and δ = 3.6 ppm (PMeOx or PEtOx) and was found to be 6 % for all copolymers.

Synthesis of PMeOx-PMestOx and PEtOx-PMestOx

The PMeOx-PEI, respectively PEtOx-PEI copolymers (350 mg, 1 eq of amine groups) were dissolved in DMA (20 mL). The mixture was cooled down in an ice-water bath followed by dropwise addition of triethylamine (3 eq.) and methyl chlorosuccinate (3 eq.). The reaction mixture was purged with argon and stirred at room temperature for 48 h. All volatiles were then removed under reduced pressure; the residue was dissolved in distilled water and purified by dialysis (MWCO 3.5 kDa). PMeOx-PMestOx, respectively PEtOx-PMestOx copolymers were recovered by freeze-drying as colorless solids (yield 82 - 91 %).

Synthesis of hydrazone-containing polymer carriers MH1-3, EH1-3

The PMeOx-PMestOx, respectively PEtOx-PMestOx copolymers (280 mg) were dissolved in the mixture of anhydrous methanol (4 mL) and hydrazine hydrate (1 mL) and were stirred at room temperature overnight. The volatiles were then removed under reduced pressure; the residue was dissolved in methanol and purified by gel filtration using a Sephadex LH-20 column with methanol as eluent. The hydrazide-containing polymer carriers (MH1-3, EH1-3) were obtained as colorless solids (yield 76 - 89 %).

Synthesis of PAOx-doxorubicin conjugates

A solution of the hydrazide-containing copolymer (MH2-3, EH2-3, 100 mg), doxorubicin hydrochloride (12 mg for MD1-2 and ED1-2, 17 mg for MD3 and ED3, respectively 25 mg for MD4 and ED4) and glacial acetic acid (30 μL) was vortexed in methanol (300 μL) at room temperature in the dark for three days. The conjugate was then isolated by gel filtration on Sephadex LH-20 column using methanol as an eluent, to obtain 85 - 106 mg of conjugates MD1-4, respectively ED1-4, as red solids.

Synthesis of PAOx-Atto 655 conjugates

A solution of the hydrazide-containing copolymer (MH2-3, EH2-3, 5 mg for uptake comparison in Figure 6A, B, respectively 20 mg for measurements in presence of inhibitors in Figure 6C, D), Atto 655 NHS ester (0.25 mg) and triethylamine (1 µL) in DMA (1 mL) was vortexed at room temperature overnight. The reaction mixture was evaporated under reduced pressure, dissolved in methanol (0.5 mL) and separated using a Sephadex LH-20 column with methanol as a mobile phase. The PAOx-Atto 655 conjugates were obtained as blue powders.

Synthesis of PAOx-biotin conjugates

A solution of the hydrazide-containing copolymer (MH1-3, EH1-3, 20 mg), biotin (0.5 mg), (benzotriazol-1-yl-oxytripyrrolidinophosphonium hexafluorophosphate) (PyBOP, 1 mg) and triethylamine (2 µL) in DMA (1 mL) was vortexed at room temperature overnight. The reaction mixture was evaporated under reduced pressure, dissolved in methanol (0.5 mL) and separated using a Sephadex LH-20 column with methanol as a mobile phase. The PAOx-biotin conjugates were obtained as colorless powders.

Characterization of polymers and polymer conjugates

Size exclusion chromatography (SEC) was used to determine the molar masses (M_w - weight-averaged molar mass, M_n - number-averaged molar mass) and the dispersity ($Đ = M_w/M_n$) of the prepared polymers. This was performed using an HPLC Ultimate 3000 system (Dionex, USA) equipped with an SEC column (TSKgel SuperAW3000 150 × 6 mm, 4 µm. Three detectors, UV/Vis, refractive index (RI) Optilab®-rEX and multi-angle light scattering (MALS) DAWN EOS (Wyatt Technology Co., USA) were employed; with a methanol and sodium acetate buffer (0.3 M, pH 6.5) mixture (80:20 vol%, flow rate of 0.5 mL/min) as mobile phase. The molar mass of doxorubicin-loaded conjugates was determined using low-dispersity PEtOx standards. Successful conjugation of doxorubicin, respectively Atto655 was confirmed by SEC with UV-VIS detection at 488 nm, respectively 663 nm by an absence of a low molar mass peak in the chromatogram, as well as by the high-performance liquid chromatography (HPLC) analyses. This was performed with HPLC Ultimate 3000 system (Dionex, USA) using a reverse-phase column (Chromolith Performance RP-18e 100 × 4.6 mm, Merck, Germany) and UV detection at 488 nm. Nuclear magnetic resonance (NMR) spectra were measured with a Bruker Advance MSL 400 MHz NMR spectrometer. All chemical shifts are given in ppm. The DOSY measurements were performed with a 5 mm dual 1H/31P Diff30 probe and a 40 A gradient amplifier, providing a maximum gradient strength of 11.8 T m^{-1}. The spectra were

acquired with the Diff suite package integrated in Topspin 3.2 by using a double-stimulated echo pulse sequence to compensate for possible convection during the measurements. Dynamic light scattering (DLS) measurements were used to measure hydrodynamic diameters (D_h) of prepared polymers using a Zetasizer NanoZS instrument, Model ZEN3600 (Malvern Instruments, UK). The polymer samples (c_{pol} = 2 mg mL^{-1}) in phosphate buffer-saline (PBS, pH = 7.4) were filtered through a 0.22 µm PTFE syringe filter before the measurement. The apparent hydrodynamic diameter of polymers, D_h, was determined at a scattering angle of θ = 173° and the DTS (Nano) program was used to evaluate the data. The solubility of the conjugates was tested by their dissolution in PBS (pH 7.4) at room temperature. The doxorubicin content in the conjugates was measured by UV–VIS spectrometry in water at 4 °C (ε = 9 800 l mol^{-1} cm^{-1}; λ = 488 nm). To assess the pH-responsive release profiles of doxorubicin from them, the respective polymer conjugates (2 mg) were dissolved in the phosphate buffer saline (1 mL, 150 mM, pH 7.4), respectively the acetate buffer (1 mL, 150 mM, pH 5.0) and incubated at 37 °C. In predetermined time intervals, samples (20 µL) were taken and analyzed by SEC with UV-detection (λ = 488 nm) as described before [44]. All measurements were performed in triplicates.

Biolayer interferometry

Biolayer interferometry experiments were performed using an Octet RED96 system (Pall FortéBio). For all experiments, streptavidin-coated sensors were used (Pall FortéBio) together with black flat bottom 96 well plates (Greiner). Before starting the experiment, biosensors were hydrated with PBS (+ Ca^{2+} + Mg^{2+}) for at least ten minutes. A 1 µM stock solution was prepared for all the different biotinylated polymers (MH1-3, EH1-3) in PBS (+ Ca^{2+} + Mg^{2+}). A 10 % stock solution of plasma and serum was also prepared in PBS (+ Ca^{2+} + Mg^{2+}). The assay was performed in a black flat-bottom 96-well plate using an Octed RED96 system (Pall Fortébio). First, a baseline was recorded in PBS (+ Ca^{2+} + Mg^{2+}) for 60 seconds. The different polymers were loaded onto the streptavidin-coated sensors for the next 300 seconds, followed by a washing step for 30 seconds in the same buffer as the baseline. Before recording the association of either plasma or serum, a second baseline was performed for 120 seconds in PBS (+ Ca^{2+} + Mg^{2+}). Finally, dissociation was recorded for 600 seconds in the same buffer as the second baseline.

In vitro cell experiments

Cell culture

B16 murine melanoma and SKOV-3 human ovarian cancer cells were cultured in DMEM supplemented with 10% FBS, 2 mM L-glutamine, 50 µg/mL streptomycin and 50 units/mL penicillin. Cells were incubated in a controlled, sterile environment at 37°C, 95% relative humidity and 5% CO_2.

Cell uptake

Cell uptake of the PAOx-Atto 655 conjugates was quantified by flow cytometry. B16.OVA cells were seeded in 24-well plates (150 000 cells per well, suspended in 800 µL cell medium) and incubated overnight. Next, 200 µL of PAOx-Atto 655 conjugates MH2-3 and EH2-3 solubilized in PBS was added per well, resulting in overall concentrations of 1, 0.25 and 0.05 mg/mL. The samples were incubated for 24h to allow for cellular uptake. 2 wells were treated with PBS to serve as a reference. After incubation, the wells were aspirated and washed with 1 mL of PBS. After removal of the PBS, 500 µL of cell dissociation buffer was added to the wells, followed by incubation until complete detachment of the cells was achieved. The cell suspensions were transferred to Eppendorf Safe-Lock tubes and centrifuged (350 g, 15 min, 4 °C). The supernatant was aspirated and the cell pellets were resuspended in 300 µL of PBS and kept on ice to maintain cell integrity. Flow cytometry was performed using a BD Accuri C6 (BD Biosciences). The data were analyzed using the FlowJo software package.

The uptake measurements in presence of inhibitors of specific internalization pathways were performed in a similar way as described above. Per well, 150 000 B16.OVA cells were seeded in 600 µL cell medium and incubated overnight. 1 hour before adding the polymer solutions, 200 µL of one of the following inhibitor solutions in PBS was added: filipin III (50 µg/mL), cytochalasin D (50 µg/mL), chlorpromazine (50 µg/mL), genistein (250 µg/mL) or rottlerin (125 mg/mL). The same volume and concentration of polymer solutions were used as mentioned before, resulting in the same overall concentrations. After 4 hours incubation, the cells were washed and their fluorescence measured and analyzed as previously described.

Intracellular fate

SKOV-3 cells were seeded in WillCo 35 mm glass-bottom dishes (7 500 cells per dish, suspended in 200 µL cell medium) and incubated overnight. The next day, 30 µL of PAOx-

doxorubicin conjugates (MD1-2 and ED1-2) were added to the wells. All samples were prepared in PBS to contain 50 ng doxorubicin per mL. The dishes were incubated for 24h before fixation, using 4% PFA. All samples were washed with PBS and stained with Hoechst and Phalloidin-iFluor 488 Reagent. This staining solution was prepared by adding 20 µL of 1 mg/mL Hoechst stock solution and 50 µL of a 300 units/mL Phalloidin-iFluor 488 Reagent stock solution to 2 mL PBS. Following another washing step, the cells were imaged using a Zeiss LSM710 microscope with a 40X, 0.95 NA objective.

Cytotoxicity

In vitro cytotoxicity was determined by MTT assay. B16 cells were seeded in 96-well plates (10 000 cells per well, suspended in 200 µL cell medium) and incubated overnight. The next day, 50 µL formulation, DMSO (positive control = 0% viability) or PBS (negative control = 100% viability) was added to the wells, followed by a 72h incubation period. 12 formulations of soluble doxorubicin, MD1-4 and ED1-3 each were prepared in PBS with doxorubicin concentrations ranging from 500 µg/mL to 2.5 ng/mL. After 72 hours, the medium was aspirated and the cells were washed with 200 µL PBS. After aspiration, 100 µL MTT reagent solution was added to each well and the cells were incubated for 2.5 hours. The MTT reagent solution was prepared by dissolving 100 mg thiazolyl blue tetrazolium bromide in 20 mL PBS, followed by membrane filtration (0.22 µm) and 5-fold dilution in DMEM. After 2.5 hours, the medium was aspirated and the formed formazan crystals were dissolved in 50 µL DMSO. The absorbance of each well was measured at 590 nm. The absorbance of the blank wells was used as a positive control and thus subtracted from all values.

Statistics

Significance was determined by the Student's-test (for a two-tailed distribution) using the GraphPad Prism 6.0 software package.

RESULTS AND DISCUSSION

A series of PMeOx-doxorubicin conjugates MD1-4 was synthesized using the approach depicted in **Figures 2** and **4**. Conjugates of two different sizes were prepared. The lower molar mass conjugate (~30 kDa) has a size of ~7.5 nm, which is well below the renal threshold allowing rapid elimination by the kidneys. The higher molar mass conjugates (~45 kDa) have a size of 9-10 nm, which is slightly below the renal threshold, while being large enough to be

effectively accumulated in the tumor by EPR effect, leading to the increased anti-cancer activity. To enhance the scope of this work, a series of analogous doxorubicin conjugates based on a PEtOx carrier was prepared in order to critically compare both conjugates mainly differing in the polymer carrier structure. Note that these PEtOx-doxorubicin conjugates were previously shown to have similar *in vivo* antitumor efficacy as PHPMA-doxorubicin conjugates that successfully finished Phase 2 clinical trials [45, 46]. The starting compounds for the synthesis were the respective homopolymers (PMeOx1-3 and PEtOx1-3, **Table S1**). While the lower-molar mass PMeOx1 (10 kDa), PMeOx2 (28 kDa), as well as PEtOx1-3 (11 - 45 kDa), were prepared by cationic ring-opening polymerization (CROP) of their respective monomers, the higher-molar mass PMeOx3 (39 kDa) was synthesized from PEtOx3 via full side-chain hydrolysis and acetylation of the resulting linear polyethyleneimine (PEI) as described recently [43]. This method was preferred for the synthesis of high molar mass PMeOx over the standard CROP of MeOx as the latter yielded shorter polymers with a broad dispersity due to extensive chain-transfers. In the next step, the homopolymers were subjected to controlled partial hydrolysis of their side chains, leading to the PMeOx-PEI, respectively PEtOx-PEI copolymers with 6 % of the ethyleneimine units, as determined by ^{1}H NMR spectroscopy (**Figure 2**). These secondary amines were then re-acylated by an excess of methyl chlorosuccinate to obtain methyl ester-containing copolymers PMeOx-PMestOx, respectively PEtOx-PMestOx. This approach was selected as it leads to the random distribution of the functional groups along the polymer compared to the standard statistical copolymerization of MeOx (respectively EtOx) with methyl ester-containing oxazoline monomer (*i.e.*, 2-methoxycarboxyethyl-2-oxazoline), that leads to, slight, gradient copolymer structures [47, 48]. Finally, the methyl ester groups were converted to acylhydrazides by reaction with hydrazine to provide polymer carriers MH1-3, respectively EH1-3 containing 6 mol% of hydrazide groups. The successful hydrazinolysis was confirmed by ^{1}H NMR spectroscopy from the disappearance of the methyl ester peak at 3.7 ppm. The polymer carriers were well-defined, with relatively low dispersity ($Đ < 1.25$) and molar mass in the range of 10 – 47 kDa (**Table 1**, **Figure S2**).

Table 1. Characteristics of hydrazide-containing polymer carriers.

Polymer carrier	Starting polymer	M_n (kDa)[a]	M_w (kDa)[a]	$Đ$[a]
MH1	PMeOx1	10.4	12.0	1.14
MH2	PMeOx2	24.9	30.4	1.22
MH3	PMeOx3	35.1	41.0	1.17

EH1	PEtOx1	11.6	12.4	1.07
EH2	PEtOx2	23.2	25.8	1.11
EH3	PEtOx3	40.8	47.3	1.16

[a]Determined by SEC.

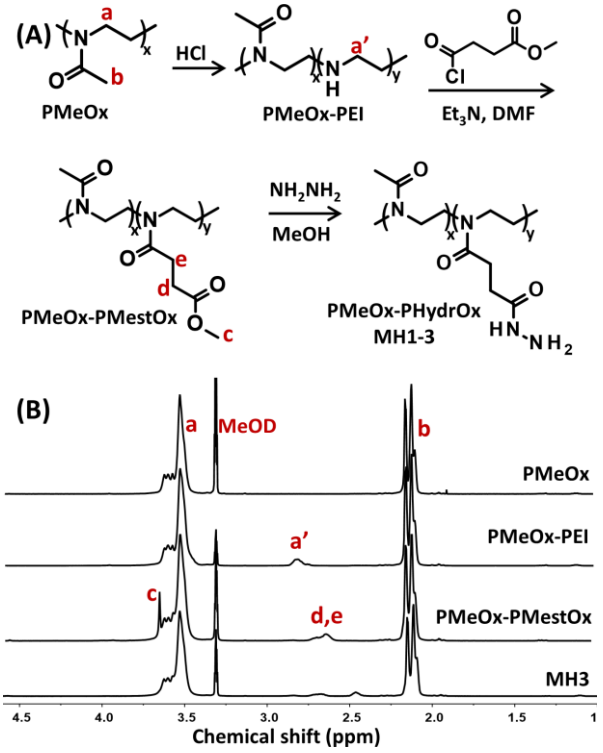

Figure 2. Synthesis of hydrazide-containing polymer carriers MH1-3. Synthetic scheme (A). ^{1}H NMR spectra of (top to bottom) PMeOx3, PMeOx-PEI3, PMeOx-PMestOx3 and MH3 in CD_3OD.

The antifouling properties of the synthesized polymer carriers were studied by biolayer interferometry (BLI) [49]. Streptavidin-coated sensors were loaded with biotin-functionalized copolymers MH1-3, respectively EH1-3. Polymer-free sensors were used as control. The sensors were then challenged with 10 % human plasma (**Figure 3A**), respectively 10 % human serum (**Figure 3B**) for 600 s, followed by recording the BLI sensorgrams to assess the protein adsorption. Afterward, the sensors were washed with PBS to study the desorption. In the very beginning, slightly higher protein adsorption was observed for PMeOx-coated sensors. However, with the extended incubation time, a considerably higher amount of adsorbed proteins and, therefore, inferior anti-fouling properties was found in PEtOx-coated surfaces. These results are in line with the previously reported anti-fouling measurements of low molar mass

polymer brushes by spectroscopic ellipsometry or surface plasmon resonance spectrometry and can be explained by higher hydrophobicity of PEtOx resulting in a lower degree of polymer hydration [40, 50]. The difference in anti-fouling properties between PMeOx and PEtOx was more distinctive in plasma, presumably due to the enhanced association of PEtOx with blood clotting proteins (i.e., fibrinogens) that are absent in serum. The protein association was dependent on the polymer length, as well. In plasma, the shortest polymers (i.e., MH1 and EH1) showed better anti-fouling properties compared to their longer analogues, while the opposite effect is observed in serum. To conclude, we demonstrated that PMeOx shows better anti-fouling properties than PEtOx even at higher molar masses, suggesting its superior potential for drug delivery applications.

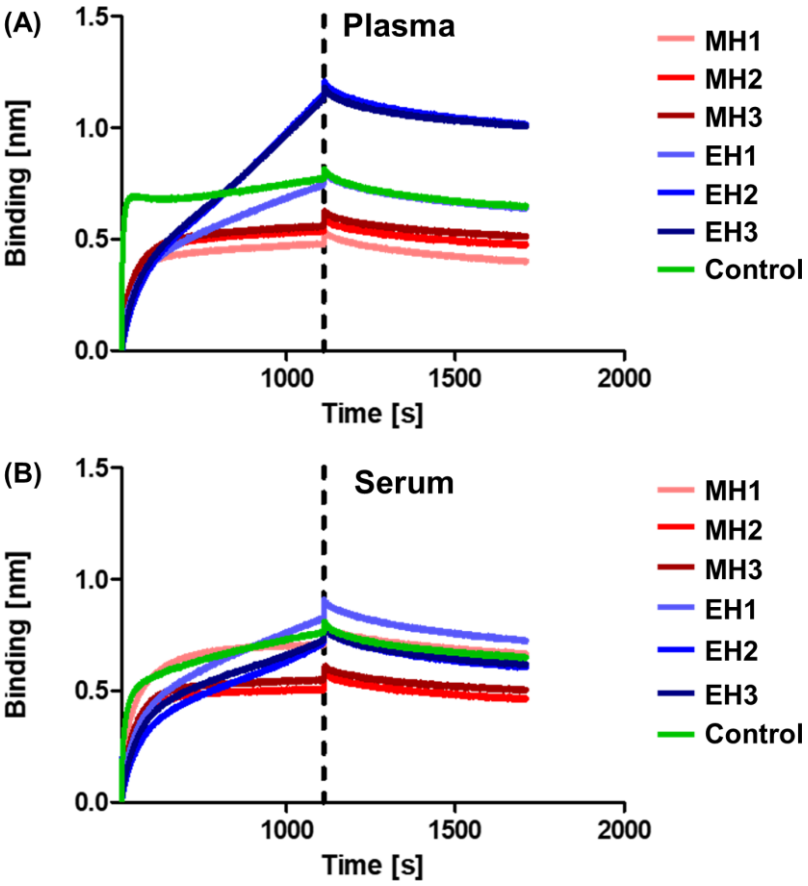

Figure 3. Biolayer interferometry (BLI) sensorgrams showing protein adsorption and desorption (after 1100 s) of PAOx-coated sensors, respectively polymer-free control when challenged with 10 % human plasma (A), or 10 % human serum (B) for 600 s.

Anti-cancer polymer conjugates with doxorubicin linked via pH-responsive hydrazone linker were synthesized by acid-catalyzed reaction of doxorubicin hydrochloride with the hydrazide-containing polymer carriers (**Figure 4, Table 2**). The shortest polymer carriers (MH1, EH1)

were not used for the conjugation, as their molar mass (ca 10 kDa) is insufficient for the EPR-based tumor accumulation. The conjugates differed in the structure and size of the polymer carrier, and the drug loading. A series of conjugates with similar drug loading (7.1-8.4 wt.%) but different polymer carrier was prepared. These were based on the lower-molar mass (conjugate MD1), respectively higher-molar mass PMeOx carrier (MD2), and their PEtOx analogs (ED1, respectively ED2). Furthermore, conjugates of higher molar mass polymers with higher doxorubicin loading were prepared (MD3-4, respectively ED3-4). The molar mass of the prepared conjugates was slightly higher compared to the drug-free polymer carriers, while their dispersity remained low (**Figure S3**). Several key biological characteristics of polymer conjugates, such as plasma circulation half-life and tumor uptake, depend on their hydrodynamic size rather than molar mass [51]. Therefore, we measured the hydrodynamic diameter (D_h) of the prepared conjugates by dynamic light scattering (DLS). The size of the lower molar mass conjugates (MD1 and ED1) was ~7.5 nm, while the D_h of the higher molar mass conjugates (MD2-4 and ED2-3) was in the range of 9.0 - 9.5 nm. The successful conjugation, as well as the absence of free doxorubicin, was confirmed by HPLC and SEC chromatography with UV-VIS detection (λ = 488 nm, **Figure S4**). Furthermore, the diffusion ordered spectroscopy (DOSY) NMR of the conjugates revealed that the diffusion coefficients of the doxorubicin peaks match those of the polymer peaks and therefore proves the effective conjugation (**Figure 4B**).

Table 2. Characteristics of polymer-doxorubicin conjugates.

Conjugate	Polymer carrier	M_n (kDa)[a]	M_w (kDa)[a]	$Đ$[a]	D_h (nm)[b]	Doxorubicin content (wt.%)[c]	PBS solubility[d]
MD1	MH2	26.3	32.9	1.25	7.8	7.1	Soluble
MD2	MH3	39.7	47.2	1.19	9.2	8.1	Soluble
MD3	MH3	37.5	46.1	1.23	9.0	12.6	Soluble
MD4	MH3	40.2	47.4	1.18	9.5	15.2	Soluble
ED1	EH2	25.9	29.3	1.13	7.3	8.0	Soluble
ED2	EH3	42.5	52.7	1.24	9.4	8.4	Soluble
ED3	EH3	41.8	49.7	1.19	9.1	10.7	Soluble

ED4	EH3	43.0	51.6	1.2	n.d.[e]	15.6	Insoluble

[a]Determined by SEC. [b]Determined by DLS in PBS [c]Determined by UV-VIS spectroscopy. [d]Solubility of conjugates (5 mg mL^{-1}) in PBS (pH = 7.4) at 37 °C. [e]Not determined.

The higher hydrophilicity of PMeOx ensures higher maximal drug loading in its conjugates, which might improve the *in vivo* anti-cancer efficiency of such conjugates, as demonstrated for the PHPMA-doxorubicin conjugates [52]. All the prepared PMeOx-Dox conjugates (with doxorubicin loading up to 15.2 wt.%) were easily soluble in PBS (pH = 7.4), while dissolution of PEtOx-Dox conjugates was substantially slower and the conjugate with the highest doxorubicin loading (ED4, loading 15.6 wt.%) was not soluble. This difference underlines the potential of PMeOx as a platform for the construction of high drug-loading drug-delivery systems.

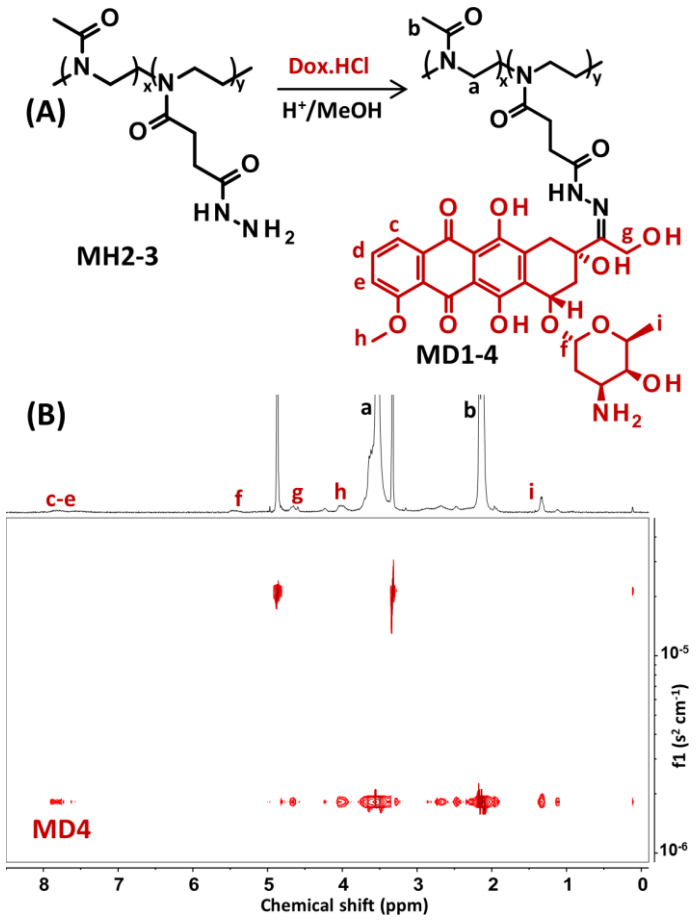

Figure 4. Conjugation of doxorubicin to PMeOx carrier resulting in conjugates MD1-4 (A). ^{1}H DOSY spectra of conjugate MD4 in CD_3OD (B).

All conjugates show a pH-responsive release of doxorubicin (**Figure 5**). At physiological pH 7.4, which mimics the conditions during the plasma circulation, the conjugates are stable, with less than 5 % of doxorubicin release after 24 h of incubation. On the other hand, doxorubicin is rapidly released at acidic pH 5.0, simulating the conditions in endosomes after the cellular internalization, with ~90 % of Dox released after 24 h. This release is substantially faster compared to the reported micellar conjugates with doxorubicin attached to the polymer by hydrazone bonds in the hydrophobic core with limited hydration [53]. Such strong pH-responsiveness of drug release ensures both safety during the blood circulation and high anti-cancer efficiency upon the cellular internalization. There was no statistically significant difference between the release kinetics of all prepared conjugates, which confirms that the release rate depends mainly on the close chemical environment of the hydrazone linker [38].

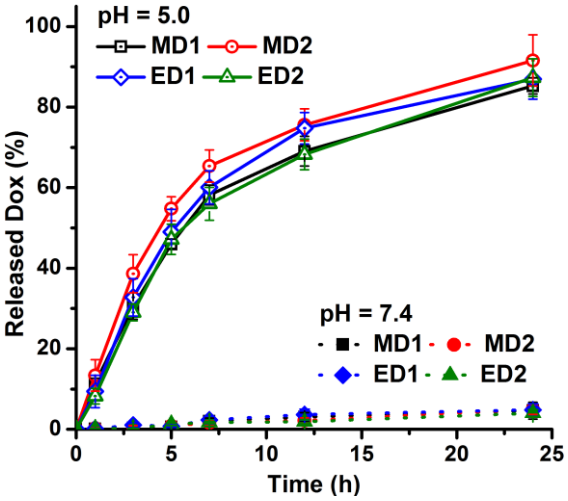

Figure 5. Release profiles of doxorubicin from the prepared conjugates in buffered media at 37 °C. Data points and error bars represent mean value and SD, respectively(n=3).

In vitro testing of the drug-free fluorescently labeled PAOx-Atto 655 conjugates on B16 murine melanoma cells showed preferential uptake of the PMeOx carrier when compared to the PEtOx carrier. When comparing different sizes of the same polymer carrier, the lower-molar mass conjugate resulted in higher cellular uptake, independent of the polymer carrier. These results were consistent for all concentrations tested (**Figure 6A**). The more pronounced uptake of smaller polymers is in line with the uptake studies of fluorescently labeled PHPMA [54, 55]. The difference in the internalization efficiency between both polymer types could be explained by a difference in cellular uptake mechanisms [56]. As the uptake mechanism of PAOx was not reported yet, we repeated the internalization experiments using different uptake inhibitors, namely chlorpromazine (inhibiting the clathrin-mediated endocytosis), filipin III, genistein

(both inhibiting the caveolar endocytic pathway), cytochalasin D and rottlerin (both inhibiting macropinocytosis) [57]. These preliminary uptake screening experiments suggest that internalization of all copolymers proceeds via clathrin-mediated endocytosis, which is in line with the mechanism reported for other linear hydrophilic polymers (e.g., PHPMA) [58]. Furthermore, the less pronounced uptake inhibition by rottlerin suggests macropinocytosis as an additional uptake pathway. Slightly more macropinocytosis was observed for more hydrophilic PMeOx, which can contribute to its higher uptake. Remarkably, the addition of cytochalasin D resulted in significant polymer uptake enhancement caused by disruption of actin. This phenomenon was previously shown to be cell-line specific [59]. Finally, the caveolae-mediated internalization mechanism seems to be less probable due to the negligible uptake inhibition by filipin III and genistein. This is in line with previous reports showing caveolar mechanism to be less likely for uptake of particles smaller than 200 nm [60]. To conclude, the internalization pathways of hydrophilic poly(2-oxazoline)s follow similar trends as other hydrophilic polymers, e.g., PHPMA. Even though the reason for higher cellular uptake of PMeOx compared to PEtOx remains unclear it demonstrates the potential of PMeOx as a versatile platform for the construction of drug delivery systems.

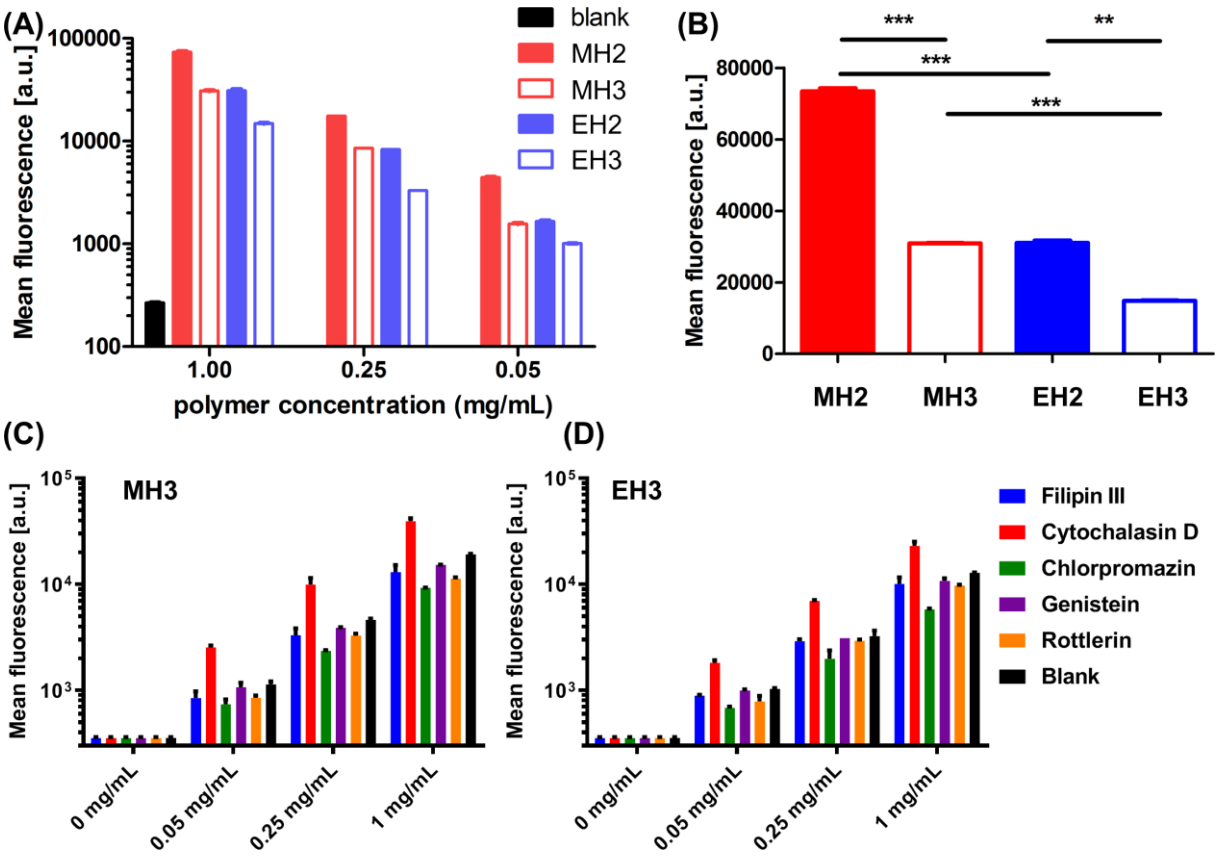

Figure 6. (A) Mean fluorescence of B16 cells, incubated for 24 hours with PAOx-Atto 655 conjugates at concentrations of 1, 0.25 and 0.05 mg/mL. (B) Detailed results for conjugates at 1 mg/mL. Cell uptake of MH3 (C), respectively EH3 (D) determined in the presence of selective internalization mechanism inhibitors. Data points and error bars represent mean value and SD, respectively. Student's t-tests, n=2, **: $p < 0.01$, ***: $p < 0.001$ (n=3).

The intracellular fate of the PAOx-doxorubicin conjugates after uptake by SKOV-3 human ovarian cancer cells was visualized by confocal microscopy. As B16 cells tended to succumb rapidly to the toxicity of DOX, we opted to perform confocal microscopy imaging on SKOV-3 cells which are more resistant to DOX and, owing to their thin stretched morphology, allow for high quality imaging. Not only did all tested conjugates display good cellular uptake (as evidenced by the punctuated pattern of red fluorescence), extensive accumulation of released doxorubicin in the nucleus could be clearly observed. This demonstrates the suitability of the hydrazone linker for acid-induced controlled release of the drug load after endosomal uptake (**Figure 7**).

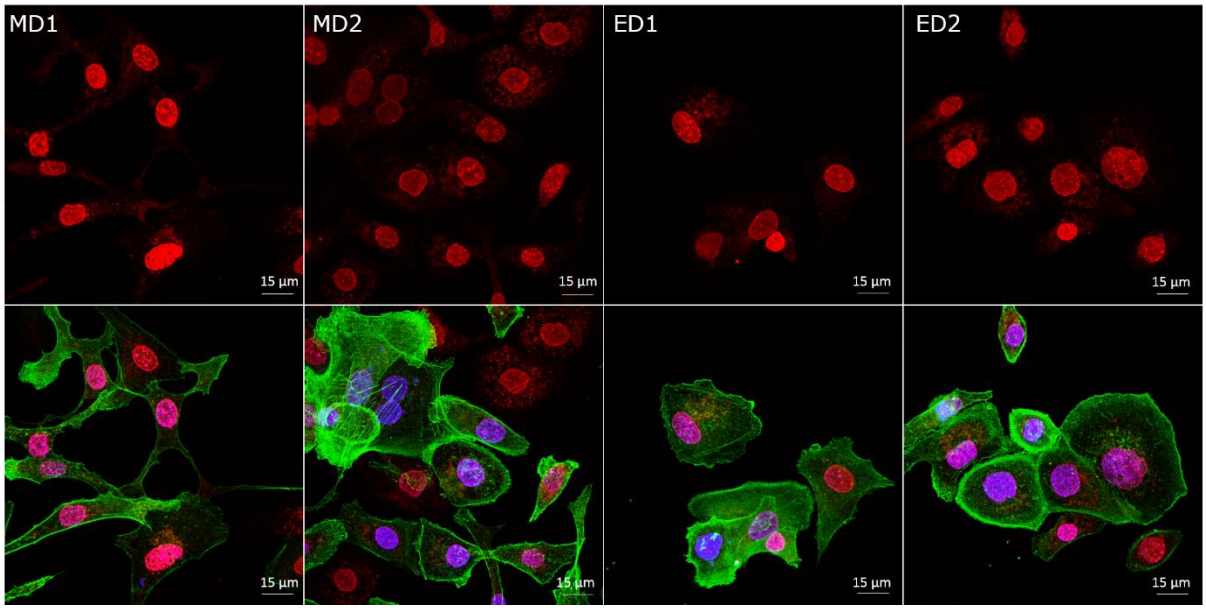

Figure 7. Confocal images of SKOV-3 cells incubated with PAOx-doxorubicin conjugates MD1-2 and ED1-2 for 24 hours. Doxorubicin is visualized in red. Cell nuclei and actin are shown in blue and green respectively. Images represent a maximum intensity projection (MIP) constructed from a 10-15 slice z-stack.

When comparing the cytotoxic effect of the PAOx-doxorubicin conjugates to free, unconjugated doxorubicin, very little loss of activity was observed. Although the difference was small, the PMeOx-doxorubicin conjugates proved to be slightly more cytotoxic than their

PEtOx-doxorubicin counterparts. The size effect observed during flow cytometry testing did not appear to affect the cytotoxicity as all PMeOx and all PEtOx conjugates with different molar mass and different drug loading showed very similar cytotoxicity (**Figure 8**). To summarize, PMeOx outperforms PEtOx in most of the measured biological parameters and therefore represents a polymer of choice for construction of PAOx-based drug delivery conjugates.

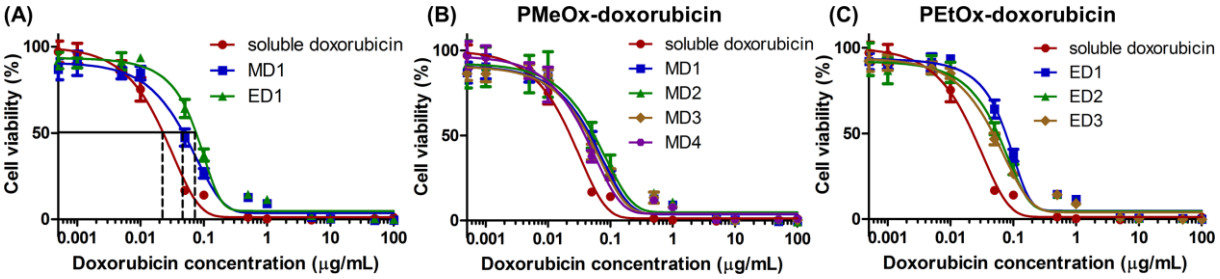

Figure 8. In vitro cytotoxicity evaluation on B16 cells after 72 hours of incubation with soluble doxorubicin and polymer-doxorubicin conjugates (n=6). Comparison of lower molecular weight PMeOx-doxorubicin with PEtOx-doxorubicin and free doxorubicin (A), cytotoxicity of PMeOx-doxorubicin (B) and PEtOx-doxorubicin (C) conjugates. For polymer conjugates, the doxorubicin concentration represents the initial concentration of polymer-bound doxorubicin. Data points and error bars represent mean value and SD, respectively (n=6).

Conclusions

Herein, we report for the first time the synthesis and *in vitro* anti-cancer properties of high molar mass drug delivery conjugates based on hydrophilic poly(2-methyl-2-oxazoline) (PMeOx) covalently conjugated with doxorubicin via acid cleavable hydrazone bonds. The conjugates show pH-responsive doxorubicin release, high cellular uptake and in vitro cytotoxicity against B16 melanoma cells. To further extend the scope of this work, we compared these properties to the analogous conjugates based on the established poly(2-ethyl-2-oxazoline) (PEtOx).

It is demonstrated that the PMeOx carrier outperforms PEtOx in most of the measured parameters. In addition to the already reported better anti-fouling properties, the more hydrophilic PMeOx also allows higher drug loadings, increased cellular uptake and higher in vitro anti-cancer effectivity. These properties, together with its synthetic versatility demonstrate the high potential of PMeOx as a platform for the synthesis of next-generation drug delivery systems. Our future work will focus on detailed *in vivo* examination of the prepared polymer conjugates to further prove their anti-cancer potential.

Associated content

The Supporting Information is available: Detailed experimental procedures and characterization of the synthesized polymers.

Author Contributions

The manuscript was written through the contributions of all authors. All authors have approved the final version of the manuscript.

Notes

RH is one of the founders of Avroxa BVBA that commercializes poly(2-oxazoline)s as Ultroxa®. The other authors have no conflicts to declare.

Acknowledgments

This work was supported by FWO and Ghent University. O.S. thanks to the funding from the FWO and European Union's Horizon 2020 research and innovation program under the Marie Skłodowska-Curie grant agreement No 665501. A.V.D., SB PhD fellow at FWO, thanks to the Research Foundation-Flanders for a Ph.D. scholarship (grant number 1S01017N).

References

[1] R. Duncan, M.J. Vicent, Polymer therapeutics-prospects for 21st century: the end of the beginning, Advanced drug delivery reviews, 65 (2013) 60-70.
[2] J. Kopeček, Polymer–drug conjugates: origins, progress to date and future directions, Advanced drug delivery reviews, 65 (2013) 49-59.
[3] N. Larson, H. Ghandehari, Polymeric conjugates for drug delivery, Chemistry of Materials, 24 (2012) 840-853.
[4] V. Torchilin, Tumor delivery of macromolecular drugs based on the EPR effect, Advanced drug delivery reviews, 63 (2011) 131-135.
[5] T. Lammers, F. Kiessling, W.E. Hennink, G. Storm, Drug targeting to tumors: principles, pitfalls and (pre-) clinical progress, Journal of controlled release, 161 (2012) 175-187.
[6] K. Ulbrich, K. Hola, V. Subr, A. Bakandritsos, J. Tucek, R. Zboril, Targeted drug delivery with polymers and magnetic nanoparticles: covalent and noncovalent approaches, release control, and clinical studies, Chemical reviews, 116 (2016) 5338-5431.
[7] J. Fang, H. Nakamura, H. Maeda, The EPR effect: unique features of tumor blood vessels for drug delivery, factors involved, and limitations and augmentation of the effect, Advanced drug delivery reviews, 63 (2011) 136-151.

[8] H. Maeda, Macromolecular therapeutics in cancer treatment: the EPR effect and beyond, Journal of Controlled Release, 164 (2012) 138-144.
[9] K. Knop, R. Hoogenboom, D. Fischer, U.S. Schubert, Poly (ethylene glycol) in drug delivery: pros and cons as well as potential alternatives, Angewandte chemie international edition, 49 (2010) 6288-6308.
[10] R.K. Gangwar, V.A. Dhumale, D. Kumari, U.T. Nakate, S. Gosavi, R.B. Sharma, S. Kale, S. Datar, Conjugation of curcumin with PVP capped gold nanoparticles for improving bioavailability, Materials Science and Engineering: C, 32 (2012) 2659-2663.
[11] R. Duncan, M.J. Vicent, Do HPMA copolymer conjugates have a future as clinically useful nanomedicines? A critical overview of current status and future opportunities, Advanced drug delivery reviews, 62 (2010) 272-282.
[12] J. Yang, J. Kopeček, Design of smart HPMA copolymer-based nanomedicines, Journal of Controlled Release, 240 (2016) 9-23.
[13] R. Hoogenboom, Poly (2-oxazoline) s: a polymer class with numerous potential applications, Angewandte Chemie International Edition, 48 (2009) 7978-7994.
[14] H. Schlaad, C. Diehl, A. Gress, M. Meyer, A.L. Demirel, Y. Nur, A. Bertin, Poly (2-oxazoline) s as smart bioinspired polymers, Macromolecular rapid communications, 31 (2010) 511-525.
[15] R. Luxenhofer, Y. Han, A. Schulz, J. Tong, Z. He, A.V. Kabanov, R. Jordan, Poly (2-oxazoline) s as Polymer Therapeutics, Macromolecular rapid communications, 33 (2012) 1613-1631.
[16] B. Verbraeken, B.D. Monnery, K. Lava, R. Hoogenboom, The chemistry of poly (2-oxazoline) s, European Polymer Journal, 88 (2017) 451-469.
[17] T. Lorson, M.M. Lübtow, E. Wegener, M.S. Haider, S. Borova, D. Nahm, R. Jordan, M. Sokolski-Papkov, A.V. Kabanov, R. Luxenhofer, Poly (2-oxazoline) s based biomaterials: A comprehensive and critical update, Biomaterials, 178 (2018) 204-280.
[18] O. Sedlacek, B.D. Monnery, S.K. Filippov, R. Hoogenboom, M. Hruby, Poly (2-Oxazoline) s–Are They More Advantageous for Biomedical Applications Than Other Polymers?, Macromolecular rapid communications, 33 (2012) 1648-1662.
[19] M. Bauer, C. Lautenschlaeger, K. Kempe, L. Tauhardt, U.S. Schubert, D. Fischer, Poly (2-ethyl-2-oxazoline) as Alternative for the Stealth Polymer Poly (ethylene glycol): Comparison of in vitro Cytotoxicity and Hemocompatibility, Macromolecular bioscience, 12 (2012) 986-998.

[20] T.X. Viegas, M.D. Bentley, J.M. Harris, Z. Fang, K. Yoon, B. Dizman, R. Weimer, A. Mero, G. Pasut, F.M. Veronese, Polyoxazoline: chemistry, properties, and applications in drug delivery, Bioconjugate chemistry, 22 (2011) 976-986.
[21] O. Sedlacek, R. Hoogenboom, Drug Delivery Systems Based on Poly (2-Oxazoline) s and Poly (2-Oxazine) s, Advanced Therapeutics, (2020) 1900168.
[22] R. Luxenhofer, A. Schulz, C. Roques, S. Li, T.K. Bronich, E.V. Batrakova, R. Jordan, A.V. Kabanov, Doubly amphiphilic poly (2-oxazoline) s as high-capacity delivery systems for hydrophobic drugs, Biomaterials, 31 (2010) 4972-4979.
[23] M. Schmidt, S. Harmuth, E.R. Barth, E. Wurm, R. Fobbe, A. Sickmann, C. Krumm, J.C. Tiller, Conjugation of ciprofloxacin with poly (2-oxazoline) s and polyethylene glycol via end groups, Bioconjugate chemistry, 26 (2015) 1950-1962.
[24] A. Mero, G. Pasut, L. Dalla Via, M.W. Fijten, U.S. Schubert, R. Hoogenboom, F.M. Veronese, Synthesis and characterization of poly (2-ethyl 2-oxazoline)-conjugates with proteins and drugs: suitable alternatives to PEG-conjugates?, Journal of Controlled Release, 125 (2008) 87-95.
[25] R.W. Moreadith, T.X. Viegas, M.D. Bentley, J.M. Harris, Z. Fang, K. Yoon, B. Dizman, R. Weimer, B.P. Rae, X. Li, Clinical development of a poly (2-oxazoline)(POZ) polymer therapeutic for the treatment of Parkinson's disease–Proof of concept of POZ as a versatile polymer platform for drug development in multiple therapeutic indications, European Polymer Journal, 88 (2017) 524-552.
[26] J.H. Lee, Y. Yeo, Controlled drug release from pharmaceutical nanocarriers, Chemical engineering science, 125 (2015) 75-84.
[27] D. Böhme, A.G. Beck-Sickinger, Drug delivery and release systems for targeted tumor therapy, Journal of Peptide Science, 21 (2015) 186-200.
[28] Q. Zhang, Z. Hou, B. Louage, D. Zhou, N. Vanparijs, B.G. De Geest, R. Hoogenboom, Acid-Labile Thermoresponsive Copolymers That Combine Fast pH-Triggered Hydrolysis and High Stability under Neutral Conditions, Angewandte Chemie International Edition, 54 (2015) 10879-10883.
[29] X. Xu, P.E. Saw, W. Tao, Y. Li, X. Ji, S. Bhasin, Y. Liu, D. Ayyash, J. Rasmussen, M. Huo, ROS-responsive polyprodrug nanoparticles for triggered drug delivery and effective cancer therapy, Advanced Materials, 29 (2017) 1700141.
[30] A. Van Driessche, A. Kocere, H. Everaert, L. Nuhn, S. Van Herck, G. Griffiths, F. Fenaroli, B.G. De Geest, pH-Sensitive Hydrazone-Linked Doxorubicin Nanogels via

Polymeric-Activated Ester Scaffolds: Synthesis, Assembly, and In Vitro and In Vivo Evaluation in Tumor-Bearing Zebrafish, Chemistry of Materials, 30 (2018) 8587-8596.
[31] B. Louage, M.J. Van Steenbergen, L. Nuhn, M.D. Risseeuw, I. Karalic, J. Winne, S. Van Calenbergh, W.E. Hennink, B.G. De Geest, Micellar paclitaxel-initiated RAFT polymer conjugates with acid-sensitive behavior, ACS Macro Letters, 6 (2017) 272-276.
[32] R. De La Rica, D. Aili, M.M. Stevens, Enzyme-responsive nanoparticles for drug release and diagnostics, Advanced drug delivery reviews, 64 (2012) 967-978.
[33] J. Kalia, R.T. Raines, Hydrolytic stability of hydrazones and oximes, Angewandte Chemie International Edition, 47 (2008) 7523-7526.
[34] T. Etrych, M. Jelínková, B. Říhová, K. Ulbrich, New HPMA copolymers containing doxorubicin bound via pH-sensitive linkage: synthesis and preliminary in vitro and in vivo biological properties, Journal of Controlled Release, 73 (2001) 89-102.
[35] O. Sedláček, M. Studenovský, D. Větvička, K. Ulbrich, M. Hrubý, Fine tuning of the pH-dependent drug release rate from polyHPMA-ellipticinium conjugates, Bioorganic & medicinal chemistry, 21 (2013) 5669-5672.
[36] B.D. Monnery, V.V. Jerca, O. Sedlacek, B. Verbraeken, R. Cavill, R. Hoogenboom, Defined High Molar Mass Poly (2-Oxazoline) s, Angewandte Chemie International Edition, 57 (2018) 15400-15404.
[37] T. Verbrugghen, B.D. Monnery, M. Glassner, S. Stroobants, R. Hoogenboom, S. Staelens, μPET imaging of the pharmacokinetic behavior of medium and high molar mass 89Zr-labeled poly (2-ethyl-2-oxazoline) in comparison to poly (ethylene glycol), Journal of Controlled Release, 235 (2016) 63-71.
[38] O. Sedlacek, B.D. Monnery, J. Mattova, J. Kucka, J. Panek, O. Janouskova, A. Hocherl, B. Verbraeken, M. Vergaelen, M. Zadinova, Poly (2-ethyl-2-oxazoline) conjugates with doxorubicin for cancer therapy: In vitro and in vivo evaluation and direct comparison to poly [N-(2-hydroxypropyl) methacrylamide] analogues, Biomaterials, 146 (2017) 1-12.
[39] B. Pidhatika, M. Rodenstein, Y. Chen, E. Rakhmatullina, A. Mühlebach, C. Acikgöz, M. Textor, R. Konradi, Comparative stability studies of poly (2-methyl-2-oxazoline) and poly (ethylene glycol) brush coatings, Biointerphases, 7 (2012) 1.
[40] G. Morgese, B. Verbraeken, S.N. Ramakrishna, Y. Gombert, E. Cavalli, J.G. Rosenboom, M. Zenobi-Wong, N.D. Spencer, R. Hoogenboom, E.M. Benetti, Chemical Design of Non-Ionic Polymer Brushes as Biointerfaces: Poly (2-oxazine) s Outperform both Poly (2-oxazoline) s and PEG, Angewandte Chemie International Edition, 57 (2018) 11667-11672.

[41] F. Wiesbrock, R. Hoogenboom, M.A. Leenen, M.A. Meier, U.S. Schubert, Investigation of the living cationic ring-opening polymerization of 2-methyl-, 2-ethyl-, 2-nonyl-, and 2-phenyl-2-oxazoline in a single-mode microwave reactor, Macromolecules, 38 (2005) 5025-5034.
[42] O. Sedlacek, O. Janouskova, B. Verbraeken, R. Hoogenboom, Straightforward Route to Superhydrophilic Poly (2-oxazoline) s via Acylation of Well-Defined Polyethylenimine, Biomacromolecules, 20 (2018) 222-230.
[43] O. Sedlacek, B.D. Monnery, R. Hoogenboom, Synthesis of defined high molar mass poly (2-methyl-2-oxazoline), Polymer Chemistry, (2019) 1286-1290.
[44] P. Chytil, M. Šírová, J.l. Kudláčová, B. Říhová, K. Ulbrich, T.s. Etrych, Bloodstream Stability Predetermines the Antitumor Efficacy of Micellar Polymer–Doxorubicin Drug Conjugates with pH-Triggered Drug Release, Molecular pharmaceutics, 15 (2018) 3654-3663.
[45] L.W. Seymour, D.R. Ferry, D.J. Kerr, D. Rea, M. Whitlock, R. Poyner, C. Boivin, S. Hesslewood, C. Twelves, R. Blackie, Phase II studies of polymer-doxorubicin (PK1, FCE28068) in the treatment of breast, lung and colorectal cancer, International journal of oncology, 34 (2009) 1629-1636.
[46] J. Yang, J. Kopeček, The light at the end of the tunnel—second generation HPMA conjugates for cancer treatment, Current opinion in colloid & interface science, 31 (2017) 30-42.
[47] M.A. Mees, R. Hoogenboom, Functional poly (2-oxazoline) s by direct amidation of methyl ester side chains, Macromolecules, 48 (2015) 3531-3538.
[48] P.J. Bouten, D. Hertsen, M. Vergaelen, B.D. Monnery, S. Catak, J.C. van Hest, V. Van Speybroeck, R. Hoogenboom, Synthesis of poly (2-oxazoline) s with side chain methyl ester functionalities: Detailed understanding of living copolymerization behavior of methyl ester containing monomers with 2-alkyl-2-oxazolines, Journal of Polymer Science Part A: Polymer Chemistry, 53 (2015) 2649-2661.
[49] A. Uvyn, R. De Coen, M. Gruijs, C.W. Tuk, J. De Vrieze, M. van Egmond, B.G. De Geest, Efficient Innate Immune Killing of Cancer Cells Triggered by Cell-Surface Anchoring of Multivalent Antibody-Recruiting Polymers, Angewandte Chemie International Edition, 58 (2019) 12988-12993.
[50] J. Svoboda, O. Sedlacek, T. Riedel, M. Hruby, O. Pop-Georgievski, Poly (2-oxazoline) s One-Pot Polymerization and Surface Coating: From Synthesis to Antifouling Properties Out-Performing Poly (ethylene oxide), Biomacromolecules, 20 (2019) 3453-3463.

[51] C. He, Y. Hu, L. Yin, C. Tang, C. Yin, Effects of particle size and surface charge on cellular uptake and biodistribution of polymeric nanoparticles, Biomaterials, 31 (2010) 3657-3666.
[52] M. Sirova, T. Mrkvan, T. Etrych, P. Chytil, P. Rossmann, M. Ibrahimova, L. Kovar, K. Ulbrich, B. Rihova, Preclinical evaluation of linear HPMA-doxorubicin conjugates with pH-sensitive drug release: efficacy, safety, and immunomodulating activity in murine model, Pharmaceutical research, 27 (2010) 200.
[53] H.S. Yoo, E.A. Lee, T.G. Park, Doxorubicin-conjugated biodegradable polymeric micelles having acid-cleavable linkages, Journal of Controlled Release, 82 (2002) 17-27.
[54] J. Callahan, P. Kopeckova, J. Kopecek, Intracellular trafficking and subcellular distribution of a large array of HPMA copolymers, Biomacromolecules, 10 (2009) 1704-1714.
[55] M. Barz, R. Luxenhofer, R. Zentel, A.V. Kabanov, The uptake of N-(2-hydroxypropyl)-methacrylamide based homo, random and block copolymers by human multi-drug resistant breast adenocarcinoma cells, Biomaterials, 30 (2009) 5682-5690.
[56] L.M. Bareford, P.W. Swaan, Endocytic mechanisms for targeted drug delivery, Advanced drug delivery reviews, 59 (2007) 748-758.
[57] S. De Koker, B.G. De Geest, S.K. Singh, R. De Rycke, T. Naessens, Y. Van Kooyk, J. Demeester, S.C. De Smedt, J. Grooten, Polyelectrolyte Microcapsules as Antigen Delivery Vehicles To Dendritic Cells: Uptake, Processing, and Cross-Presentation of Encapsulated Antigens, Angewandte Chemie International Edition, 48 (2009) 8485-8489.
[58] J. Liu, H. Bauer, J. Callahan, P. Kopečková, H. Pan, J. Kopeček, Endocytic uptake of a large array of HPMA copolymers: Elucidation into the dependence on the physicochemical characteristics, Journal of Controlled Release, 143 (2010) 71-79.
[59] L. He, E.J. Sayers, P. Watson, A.T. Jones, Contrasting roles for actin in the cellular uptake of cell penetrating peptide conjugates, Scientific reports, 8 (2018) 1-12.
[60] J. Rejman, V. Oberle, I.S. Zuhorn, D. Hoekstra, Size-dependent internalization of particles via the pathways of clathrin-and caveolae-mediated endocytosis, Biochemical journal, 377 (2004) 159-169.